

# On the exploitability of thermo-charged capacitors

Germano D'Abramo

Istituto Nazionale di Astrofisica,  
Via Fosso del Cavaliere 100,  
00133, Roma, Italy.

E-mail: `Germano.Dabramo@iasf-roma.inaf.it`

## Abstract

Recently (arXiv:0904.3188) the concept of vacuum capacitors spontaneously charged thanks to the heat absorbed from single thermal source at room temperature has been introduced, along with a detailed mathematical description of the functioning and a discussion on its main paradoxical feature that seems to violate the Second Law of Thermodynamics. In the present paper we investigate the theoretical and practical possibility of exploiting such thermo-charged capacitors as voltage/current generators: we show that if very weak provisos on the physical characteristics of the capacitors are fulfilled, then a measurable current should flow across the device, allowing the generation of potentially usable voltage, current and electric power out of a single thermal source at room temperature.

**PACS (2008):** 79.40.+z, 67.30.ef, 65.40.gd, 84.32.Tt

**Keywords:** thermionic emission · capacitors · second law of thermodynamics

## 1 Introduction

In a recent paper [1], the author introduced the concept of vacuum capacitors spontaneously charged thanks to the heat absorbed from single thermal source at room temperature, called for brevity *thermo-charged capacitors*. Further, he presented a detailed mathematical description of the basic functioning.

In the same paper, the author shows that, when the tools of the classical Thermodynamics, e.g. the Clausius entropy variation analysis, are applied to the process, a paradox seems to arise: the macroscopic behavior of a thermo-charged capacitor appears to violate the Clausius formulation of the Second Law of Thermodynamics [1].

As a matter of fact, such a result should not be seen as so weird. Although no experimental violation has been claimed to date, over the last 10-15 years an unparalleled number of challenges has been proposed against the status of the Second Law of Thermodynamics. During this period, more than 50 papers have appeared in the refereed scientific literature (see, for example Ref. [5, 6, 7, 8, 9, 10, 11, 12, 13, 14, 15, 16, 17, 18, 19, 20, 21, 23, 24]), together with a monograph entirely devoted to this subject [3]. Moreover, during the same period two international conferences on the limit of the Second Law were also held [2, 4].

The general class of recent challenges [3, 20, 24] spans from plasma [19], chemical [23], gravitational [12] and solid-state [21, 22, 24]. Currently, all these approaches appear immune to standard Second Law defenses (for a compendium of the classical defenses, see [25]) and several of them account laboratory corroboration of their underlying physical processes.

In the present paper we investigate the theoretical and practical possibility of exploiting thermo-charged capacitors as voltage/current generators. In Section 2 we review the setup of the thermo-charged capacitor and its mathematical model, as presented in [1]. In Section 3 we show that if very weak provisos on the physical characteristics of the capacitor are fulfilled, then a measurable current should flow across the device, allowing the generation of potentially usable voltage, current and electric power out of a single thermal source at room temperature.

If it were possible to experimentally and unambiguously achieve such results, then we would have an experimental violation of the Second Law in the Kelvin-Planck formulation, which parallels the alleged violation in its Clausius form discussed in [1]. In a few words, we could have a sort of *thermo-voltaic cell*.

## 2 Thermo-charged spherical capacitor

In this Section we summarize the setup and the functioning of a spherical thermo-charged capacitor, as presented in [1]

In Fig. 1 a sketched section of the vacuum spherical capacitor is shown. The outer sphere has radius  $b$  and it is made of metallic material with high work function ( $\phi_{ext.} \gg 1 \text{ eV}$ ) in order to have negligible thermionic emission

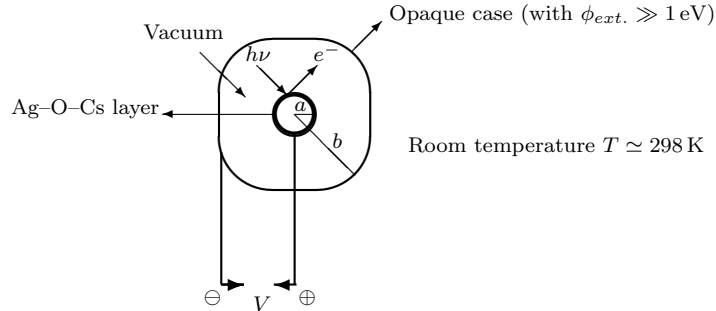


Figure 1: Scheme of the thermo-charged spherical capacitor.

at room temperature. The inner sphere has radius  $a$  and it is made of the same conductive material as the outer one, but it is covered with a layer of semiconductor Ag–O–Cs, which has a relatively low work function ( $\phi_{in.} \lesssim 0.7$  eV). It should be clear that in such cases the two thermionic fluxes, from each plate toward the other one, are always different, being the latter greater than the former and the former negligible. The capacitor should be placed inside a case at room temperature. The case must be opaque to every environmental electromagnetic disturbance (natural and man-made e.m. waves, cosmic rays and so on) in order to avoid spurious *photo*-electric emission. Moreover the inter-plates space must be under extreme vacuum (UHV).

Let us summarize how the device works. All the electrons emitted by the inner sphere, due to thermionic emission at room temperature, is collected by the outer (very low emitting) sphere, creating a macroscopic difference of potential  $V$ . Such process lasts until  $V$  is too high to be overcome by the kinetic energy  $K_e$  of the main fraction of emitted electrons (namely, when  $K_e < eV$ , where  $e$  is the charge of electron). Being the work function of the outer sphere greater than that of the inner one,  $\phi_{ext.} \gg \phi_{in.}$ , the reverse process, namely the electronic flux from the outer sphere to the inner one, may be neglected without sensibly modifying our results.

A crucial point for what follows is the behavior of the contact surface between the Ag–O–Cs layer and the conductive material of the inner sphere.

The contact surface between the metallic plate and the Ag–O–Cs layer is a well known Schottky junction (metal/n-type semiconductor). When two materials (in our case, a metal and a semiconductor) are physically joined, so as to establish a uniform chemical potential, that is a single Fermi level,

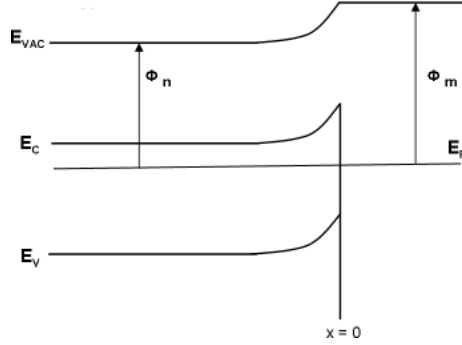


Figure 2: Band profiles of semiconductor (n) – metal (m) junction at equilibrium;  $\phi_n$  and  $\phi_m$  (with  $\phi_n < \phi_m$ ) are the work functions of semiconductor and metal, respectively ( $x = 0$  indicates the contact between surfaces).

some electrons are transferred from the material with the lesser work function  $\phi_1$  (Ag–O–Cs) to the material with the greater work function  $\phi_2$  (metal). As a result a contact potential  $V_c$  is established such that  $eV_c = \phi_2 - \phi_1$ . The energy band profiles of semiconductor-metal junction at equilibrium are shown in Fig. 2. The aspect which counts for the functioning of our device is the fact that the energy level of the vacuum for Ag–O–Cs (and that for the metallic plate) is preserved [29] far from the depletion region.

This means that whenever an electron is extracted from the Ag–O–Cs to the vacuum (towards the second sphere), and this is made always at the cost of  $\approx 0.7$  eV for what is said above, Ag–O–Cs starts to charge up positively and hence an sort of “external” reverse bias starts to form across the junction and a tiny current of electrons begins to flow from the metallic inner sphere to the Ag–O–Cs layer in order to re-establish the equilibrium (constant contact potential).

Such current flow is known as *reverse bias leakage current* (RLC). Its physical generating mechanisms are variegated and complex, and the amplitude is influenced by many factors like thickness of the depletion region, temperature, cross-sectional area and impurities of the junction, and so on. Also the amplitude of the reverse bias influences the intensity of RLC, although when the reverse bias is below the *breakdown voltage* of the junction, the current changes slowly with bias.

Usually RLC is a tiny current; it depends on the used material, but usually the *reverse leakage current density*  $j_0$  spans<sup>1</sup> from  $10^{-6}$  A/cm<sup>2</sup> to

<sup>1</sup>See, for example [32, 33, 34, 35], for some specific types of Schottky and n–p junctions. Values greater than  $10^{-6}$  A/cm<sup>2</sup> and lower than  $10^{-9}$  A/cm<sup>2</sup> are also possible with the same

$10^{-9}\text{A}/\text{cm}^2$  for reverse biases of the order of volts or tenths of volts. As it will be clear more later, if we suitably increase the contact surface between the inner metallic sphere and the Ag–O–Cs layer, namely increasing the surface of the inner sphere  $S_a$ , then the RLC can be made of the order of  $10^{-3}\text{A}$  or greater, being RLC equal to  $j_0 S_a$ . We can also be favored by junction impurities: they usually transform rectifying junctions in ohmic ones. All these issues will be treated more thoroughly in Section 3.

We now review the estimate of the voltage obtainable and the estimate of the time needed to reach such value, given the physical characteristics of the capacitor and the quantum efficiency curve  $\eta(\nu)$  of the thermionic material Ag–O–Cs (see [1]).

The capacitor is placed in a heat bath at room temperature (environment) and it is subject to the black-body radiation. Both spheres, at thermal equilibrium, emit and absorb an equal amount of radiation (Kirchhoff's law of thermal radiation), thus the amount of radiation absorbed by the inner sphere is the same emitted by that sphere according to the black-body radiation formula (Planck equation). Given the room temperature  $T$ , Planck equation provides us with the number distribution of photons absorbed as a function of their frequency.

According to the law of thermionic emission, the kinetic energy  $K_e$  of the electron emitted by the material is given by the following equation,

$$K_e = h\nu - \phi, \quad (1)$$

where  $h\nu$  is the energy of the photon with frequency  $\nu$  ( $h$  is the Planck constant) and  $\phi$  is the work function of the material. Thus, only the tail of the Planck distribution of the absorbed photons, with frequency  $\nu > \nu_0 = \phi/h$ , can contribute to the thermionic emission.

The voltage  $V$  reachable with frequency  $\nu_1$  is given by the following formula,

$$eV = h\nu_1 - \phi, \quad (2)$$

where  $eV$  is the inter-spheres potential energy, and thus,

$$\nu_1 = \frac{eV + \phi}{h}. \quad (3)$$

---

reverse bias, depending on the materials, preparation, junctions impurities and surface treatments. Usually, applied researchers and industry desire to lower the reverse leakage current in order to exalt rectifying properties of the junction for electrical and electronic applications. Here, instead, we have opposite needs.

The total number of photons per unit time  $F_p$ , with energy greater than or equal to  $h\nu_1$ , emitted and absorbed in thermal equilibrium by the inner sphere is given by the Planck equation,

$$F_p = \frac{2\pi S}{c^2} \int_{\nu_1}^{\infty} \frac{\nu^2 d\nu}{e^{\frac{h\nu}{kT}} - 1}, \quad (4)$$

where  $S$  is the sphere surface area,  $c$  is the speed of light,  $k$  is the Boltzmann constant and  $T$  the room temperature.

If  $\eta(\nu)$  is the quantum efficiency (or quantum yield) curve of the thermionic layer of the inner sphere, then the number of electrons per unit time  $F_e$ , with kinetic energy greater than or equal to  $h\nu_1 - \phi$ , emitted by the inner sphere towards the outer sphere is given by,

$$F_e = \frac{2\pi \cdot 4\pi a^2}{c^2} \int_{\nu_1}^{\infty} \frac{\eta(\nu) \nu^2 d\nu}{e^{\frac{h\nu}{kT}} - 1}, \quad (5)$$

where  $4\pi a^2$  is the surface area of the inner sphere.

For a vacuum spherical capacitor, the voltage between the spheres  $V$  and the charge on each sphere  $Q$  are linked by the following equation,

$$V = \frac{Q}{4\pi\epsilon_0} \frac{b-a}{ab}. \quad (6)$$

Now, we derive the differential equation which governs the process of thermo-charging. In the interval of time  $dt$  the charge collected by the outer sphere is given by,

$$dQ = eF_e dt = \frac{2\pi e \cdot 4\pi a^2}{c^2} \left( \int_{\frac{eV(t)+\phi}{h}}^{\infty} \frac{\eta(\nu) \nu^2 d\nu}{e^{\frac{h\nu}{kT}} - 1} \right) dt, \quad (7)$$

where we make use of eq. (3) for  $\nu_1$  and  $V(t)$  is the voltage at time  $t$ . Thus, through the differential form of eq. (6), we have,

$$dV(t) = \frac{2\pi e}{\epsilon_0 c^2} \frac{a(b-a)}{b} \left( \int_{\frac{eV(t)+\phi}{h}}^{\infty} \frac{\eta(\nu) \nu^2 d\nu}{e^{\frac{h\nu}{kT}} - 1} \right) dt, \quad (8)$$

or

$$\frac{dV(t)}{dt} = \frac{2\pi e}{\epsilon_0 c^2} \frac{a(b-a)}{b} \int_{\frac{eV(t)+\phi}{h}}^{\infty} \frac{\eta(\nu) \nu^2 d\nu}{e^{\frac{h\nu}{kT}} - 1}. \quad (9)$$

Since our aim is to maximize the generation of  $V$ , we have to choose  $a$  and  $b$  such that they maximize the geometrical factor  $a(b-a)/b$ . It is not difficult to see that the maximum is reached when  $a = b/2$ . So we have,

$$\frac{dV(t)}{dt} = \frac{\pi eb}{2\epsilon_0 c^2} \int_{\frac{eV(t)+\phi}{h}}^{\infty} \frac{\eta(\nu)\nu^2 d\nu}{e^{\frac{h\nu}{kT}} - 1}. \quad (10)$$

Unfortunately, provided that an analytical approximation of a real quantum efficiency curve  $\eta(\nu)$  exists, the previous differential equation appears to have no general, simple analytical solution.

However, a close look at the Planckian integral of eq. (10) suggests the asymptotic behavior of  $V(t)$ . Even if we do not know *a priori* how  $\eta(\nu)$  is, we know it to be a bounded function of frequency, with values between 0 and 1; usually, the higher is  $\nu$ , the closer to 1 is  $\eta(\nu)$ . Thus, independently from  $\eta(\nu)$ , a slight increase of  $V(t)$  makes the value of the Planckian integral to be smaller and smaller very fast. Heuristically, this suggests that  $V(t)$  should tend quite rapidly to an ‘asymptotic’ value (since  $\frac{dV}{dt}$  tends to 0).

In the rest of this Section we provide a numerical solution of the above differential equation for the practical case of inner sphere covered with a layer of Ag–O–Cs [26, 27, 28]. To do that we need to adopt an approximation, however: the approximation consists in the adoption of a constant value for  $\eta$ , a sort of suitable mean value  $\bar{\eta}$ .

The differential equation (10) thus becomes,

$$\frac{dV(t)}{dt} = \frac{\pi eb\bar{\eta}}{2\epsilon_0 c^2} \int_{\frac{eV(t)+\phi}{h}}^{\infty} \frac{\nu^2 d\nu}{e^{\frac{h\nu}{kT}} - 1}. \quad (11)$$

A straightforward variable substitution in the integral of eq. (11) allows to write it in its final simplified form,

$$\frac{dV(t)}{dt} = \frac{\pi eb\bar{\eta}}{2\epsilon_0 c^2} \left(\frac{kT}{h}\right)^3 \int_{\frac{eV(t)+\phi}{kT}}^{\infty} \frac{x^2 dx}{e^x - 1}. \quad (12)$$

Here we provide an exemplificative numerical solution of eq. (12), adopting the following nominal values for  $\phi$ ,  $b$ ,  $T$  and  $\bar{\eta}$ :  $\phi = 0.7$  eV,  $b = 0.20$  m,  $T = 298$  K, and  $\bar{\eta} = 10^{-5}$ . In order to make a conservative choice for the value of  $\bar{\eta}$  we note that only black-body radiation with frequency greater than  $\nu_0 = \phi/h$  can contribute to the thermionic emission. This means that for the Ag–O–Cs photo-cathode only radiation with wavelength smaller than  $\lambda_0 = hc/\phi \simeq 1700$  nm contributes to the emission. According to Fig. 1 in [28, Bates], the quantum yield of Ag–O–Cs for wavelengths smaller than  $\lambda_0$  (and thus, for frequency greater than  $\nu_0$ ) is always greater than  $10^{-5}$ . Anyway, a laboratory realization of the capacitor, together with the experimental measurement of  $V(t)$ , should provide us with a realistic estimate of  $\bar{\eta}$  for the photo-cathode Ag–O–Cs.

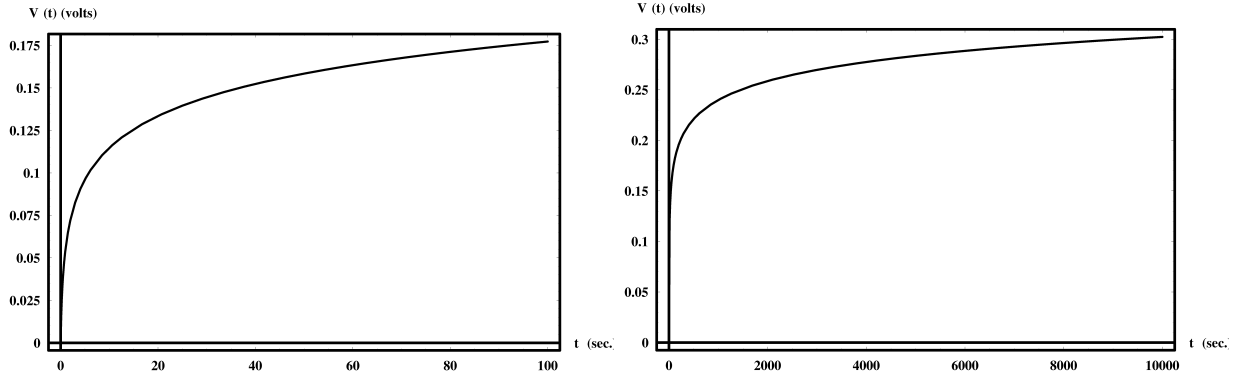


Figure 3: Thermo-charging profiles for the spherical capacitor described in the text ( $\phi = 0.7$  eV,  $b = 0.2$  m,  $T = 298$  K, and  $\bar{\eta} = 10^{-5}$ ). These two plots show with different ranges in time-scale the behavior of  $V(t)$ . Plot a) shows how only after 60 seconds the voltage of the capacitor becomes more than 0.15 volts. Instead, plot b) tells us that the voltage of the capacitor requires some hours to approach 0.3 volts.

In Fig. 3 the numerical solution of the above test it is shown. In plot (a) we could easily see how only after 60 seconds the voltage of the capacitor exceeds the value of 0.15 volts. Indeed, this is a macroscopic voltage. Instead, plot (b) tells us that the voltage of the capacitor requires some hours to approach 0.3 volts. Even in the more pessimistic scenario where  $\bar{\eta} = 10^{-8}$  we see that a macroscopic voltage should arise quite rapidly between the plates, see Fig. 4.

### 3 Discussion

In this Section we try to quantitatively show how it is possible to make a measurable current flow across the thermo-charged capacitor, once its plates are electrically shunted by a suitable resistor, and hence allowing the generation of potentially usable voltage, current and electric power out of a single thermal source at room temperature (like a classical battery). In the following, we also try to answer to some objections, which should naturally and suddenly arise against our results.

As explained in Section 2, thermionic emission produces a bias between the plates of the spherical capacitor (Fig. 3 and 4). A similar bias also arises across the junction metal/semiconductor (since the Ag–O–Cs layer charges up positively) in the inner sphere: given the nature of the metal/Ag–O–Cs junction, such bias has the characteristics of a *reverse bias*. The reverse bias causes a *reverse leakage density current*  $j_0$ , as explained in Section 2, which



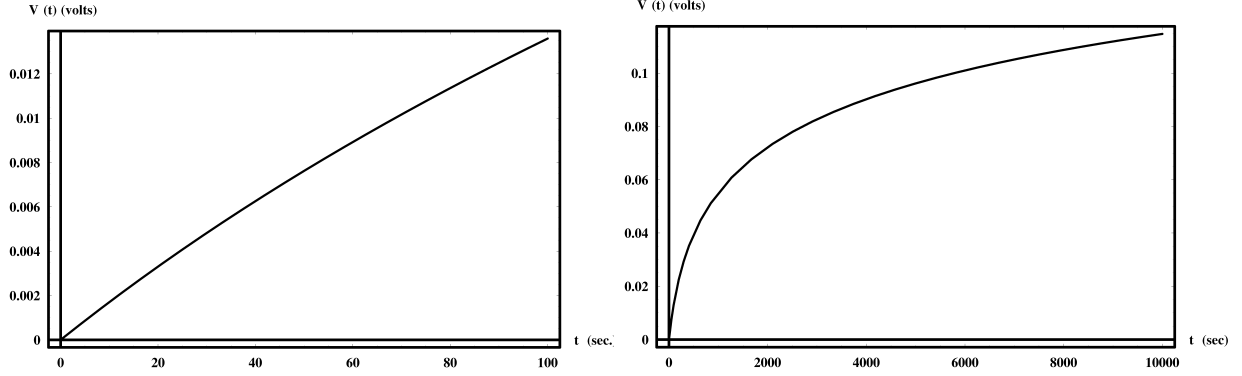


Figure 4: Thermo-charging profiles for the spherical capacitor described in the text with  $\phi = 0.7$  eV,  $b = 0.2$  m,  $T = 298$  K, and  $\bar{\eta} = 10^{-8}$ . These two plots show with different ranges in time-scale the behavior of  $V(t)$ . Plot a) shows how only after 60 seconds the voltage of the capacitor is near to 0.01 volts. Instead, plot b) tells us that the voltage of the capacitor requires some hours to become equal to 0.1 volts.

slowly transfers electrons from the inner metallic sphere to the Ag–O–Cs layer. This reverse leakage density current  $j_0$  is microscopic, usually ranging from  $10^{-6}$  A/cm<sup>2</sup> to  $10^{-9}$  A/cm<sup>2</sup> for reverse biases of the order of volts or tenths of volts, and its intensity is weakly dependent on the magnitude of the reverse bias, provided that such bias is below the breakdown voltage of the junction [32, 33, 34, 35]. As seen in the previous Section, our device is far below such voltage.

Now, the mere fact that a non zero, almost constant, reverse bias leakage density current  $j_0$  exists, although very tiny, let the thermo-charging process be potentially exploitable. As a matter of fact, if we suitably increase the surface area of the inner sphere  $S_a$  (and also that of the outer one, accordingly), then the contact area between the Ag–O–Cs layer and the metal increases. This means that in principle it is possible to obtain a macroscopic reverse leakage current (RLC) that allows a rather quick transfer of the voltage drop to both the terminal leads of the capacitor, since RLC is equal to  $j_0 S_a$ .

For the sake of though experiment, imagine to build a room-sized thermo-charged capacitor with radii  $a = 100$  cm and  $b = 200$  cm. In this case the inner sphere surface is equal to  $S_a = 4\pi a^2 \approx 10^5$  cm<sup>2</sup>. Thus, the total reverse leakage current  $j_0 S_a$  should vary between 100 mA and 0.1 mA; this is a quite macroscopic current. The thermo-charging profile for the capacitor with the following parameters  $\phi = 0.7$  eV,  $b = 2.0$  m,  $T = 298$  K, and  $\bar{\eta} = 10^{-5}$ , is represented in Fig. 5.

Let us now compare the RLC in this case with the thermionic current

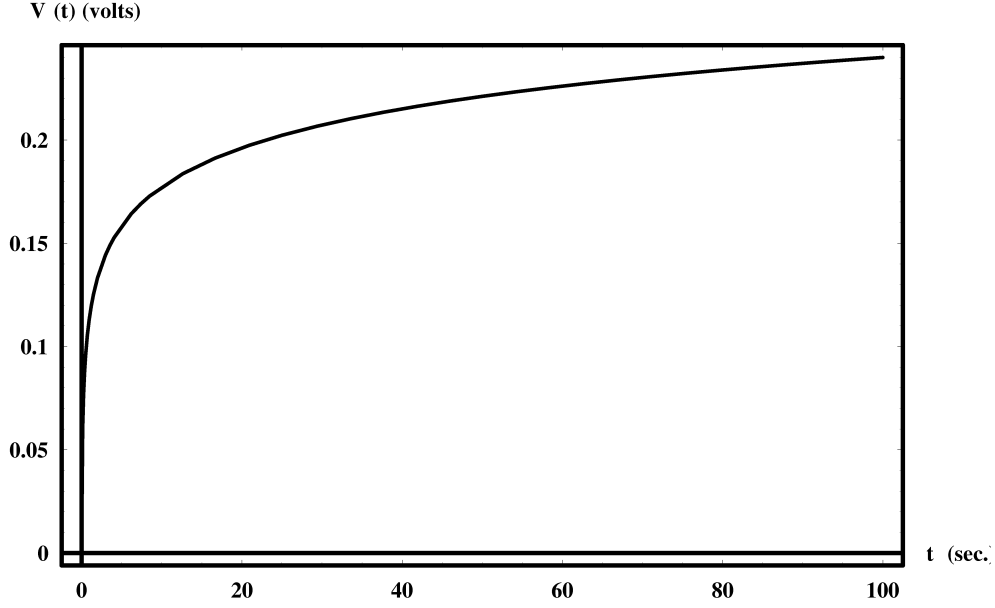


Figure 5: Thermo-charging profile for the spherical capacitor described in Section 3 with  $\phi = 0.7$  eV,  $b = 2.0$  m,  $T = 298$  K, and  $\bar{\eta} = 10^{-5}$ .

between the spheres  $i_{ti} = dQ/dt$  at  $t = 0$  s (and  $V(0) = 0$  V). It should be obvious that such value is the maximum value reachable by thermionic current during the charging process. Rearranging eq. (7) and eq. (12) we obtain,

$$i_{ti}(t) = \frac{dQ}{dt} = \frac{2\pi^2 eb^2 \bar{\eta}}{c^2} \left( \frac{kT}{h} \right)^3 \int_{\frac{eV(t)+\phi}{kT}}^{\infty} \frac{x^2 dx}{e^x - 1}, \quad (13)$$

and through numerical calculations we get  $i_{ti}(0) \approx 1.56 \times 10^{-9}$  A.

We note that  $i_{ti} \ll j_0 S_a$  and this means that the voltage drop thermally gained within the plates of the capacitor is quickly transferred to both terminal leads of the capacitor and can be directly detected through an electroscope.

But we can do better. It is possible to directly compare the reverse bias leakage density current  $j_0$  with the thermionic density current,  $j_{ti}(0)$ , obtained from eq. (13) as follows

$$j_{ti}(0) = \frac{i_{ti}(0)}{S_a} = \frac{i_{ti}(0)}{4\pi a^2} = \frac{2\pi e \bar{\eta}}{c^2} \left( \frac{kT}{h} \right)^3 \int_{\frac{\phi}{kT}}^{\infty} \frac{x^2 dx}{e^x - 1} \approx 3.11 \times 10^{-15} \text{ A/cm}^2, \quad (14)$$

assuming the maximizing condition  $a = b/2$  for  $dV/dt$  (see eq. (9)).

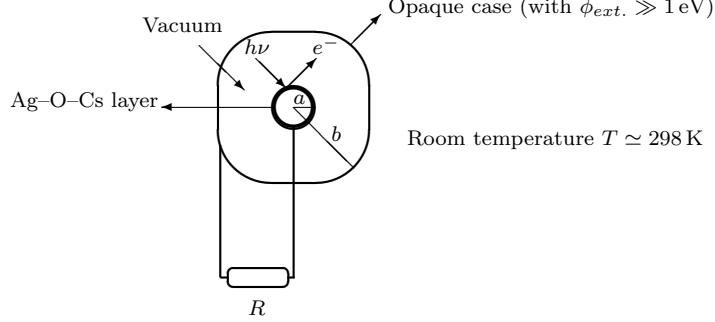


Figure 6: Thermo-charged spherical capacitor shunted by a resistor  $R$ .

Thus, for  $\phi = 0.7 \text{ eV}$ ,  $\bar{\eta} = 10^{-5}$ ,  $T = 298 \text{ K}$  and  $j_0$  in the reasonable range given above, we see from eq. (14) that  $j_0$  is always greater than  $j_{ti}(0)$ : this roughly means that the voltage drop thermally gained within the plates of the capacitor is always quickly transferred to both terminal leads of the capacitor, no matter how big or small is the capacitor. Obviously, the bigger is the capacitor, the greater will be the current “flowing” through it.

Let us now consider the capacitor of Fig. 1 shunted by a suitable resistor  $R$ . In this case the capacitor behaves like a battery shunted by a resistor, which dissipates its power through the Joule effect.

Consider the electrical circuit depicted in Fig. 6. At steady state conditions, both voltage drop  $V_s$  and current  $i_s$  across the capacitor and the resistor should be the same and should be constant in time: according to Ohm’s Law, we must have  $R = V_s/i_s$ , and this relation also gives the numerical value of the resistance  $R$  needed to have these particular values of  $V_s$  and  $i_s$ .

Given the equations of the thermo-charged capacitor described above, we also must have,

$$i_s = \frac{2\pi^2 eb^2 \bar{\eta}}{c^2} \left( \frac{kT}{h} \right)^3 \int_{\frac{eV_s + \phi}{kT}}^{\infty} \frac{x^2 dx}{e^x - 1}. \quad (15)$$

The power  $P_s$  provided by the thermo-charged capacitor is calculated as,

$$P_s = V_s i_s = \frac{2\pi^2 eb^2 \bar{\eta} V_s}{c^2} \left( \frac{kT}{h} \right)^3 \int_{\frac{eV_s + \phi}{kT}}^{\infty} \frac{x^2 dx}{e^x - 1}. \quad (16)$$

The power per unit surface of the inner sphere  $\mathcal{P}_s$  is then,

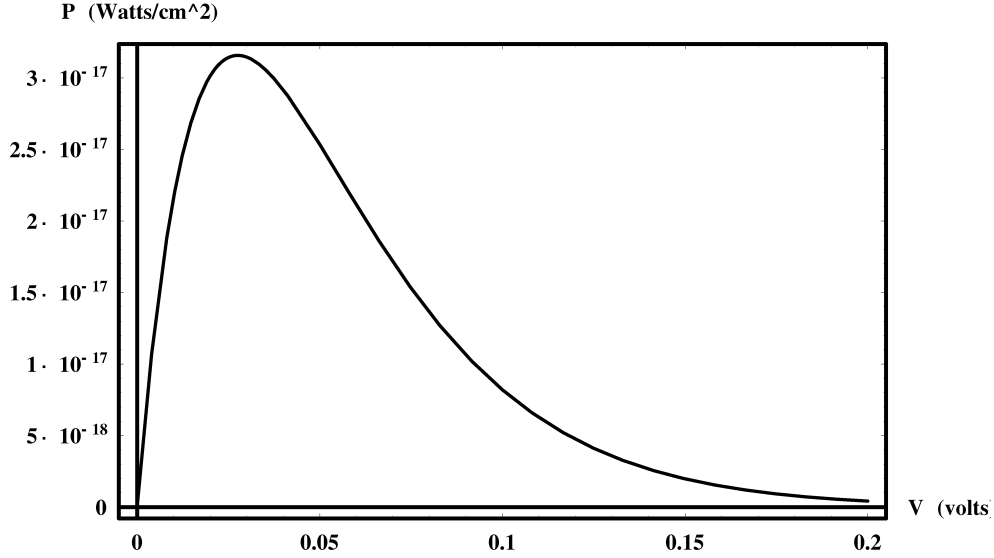


Figure 7: Power output per unit surface area of the inner sphere,  $\mathcal{P}_s$ , against voltage drop  $V_s$  of the electrical circuit thermo-charged capacitor/resistor depicted in Fig. 6.

$$\mathcal{P}_s = \frac{V_s i_s}{S_a} = \frac{2\pi e \bar{\eta} V_s}{c^2} \left( \frac{kT}{h} \right)^3 \int_{\frac{eV_s + \phi}{kT}}^{\infty} \frac{x^2 dx}{e^x - 1}. \quad (17)$$

In Fig. 7 the power  $\mathcal{P}_s$  is plotted against the steady state voltage  $V_s$ . For the capacitors described in this paper, namely that with  $a = 10$  cm,  $S_a \approx 1260$  cm<sup>2</sup> and that with  $a = 100$  cm,  $S_a \approx 10^5$  cm<sup>2</sup>, we obtain  $P_{max} \approx 4 \times 10^{-14}$  Watts and  $P_{max} \approx 4 \times 10^{-12}$  Watts, respectively. These are quite microscopic power outputs indeed, considering further that the second capacitor described has “uncomfortable” room-sized dimensions.

There are now few doubts that one of the definite results of our paper is that the thermo-charged capacitors described here are highly inefficient. Anyway, it is important to experimentally test their functioning, since if they work according the analysis done in this paper, then we would have a *reproducible* Second Law violation: then we believe that its *smallness* is a secondary problem (that can be overcome with further future research), provided that this *smallness* is not such to forbid a clear and unambiguous result with confounding environmental factors.

We have seen that the current and the power output of circuits like those depicted in Fig. 6 are microscopic, in particular if the physical dimensions of the spheres are centimetric, but the voltage drop of non-shunted capacitors

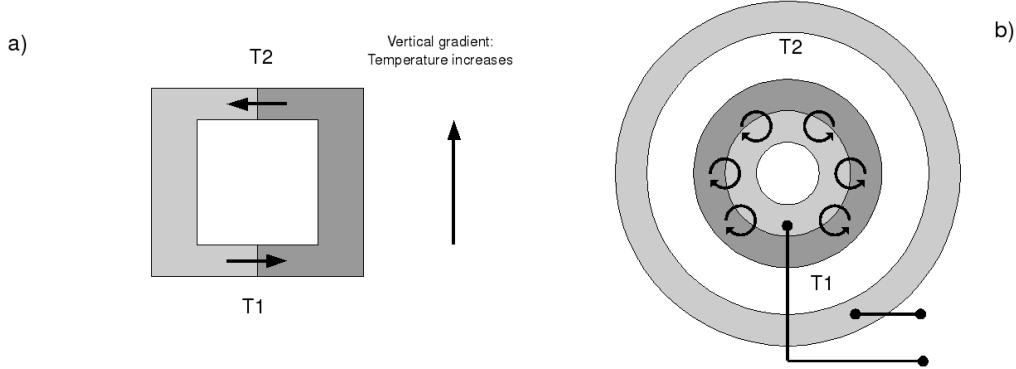


Figure 8:  $T_2 > T_1$ . a) sketch of a classical shunted thermocouple, b) a sketched section of our capacitor. The arrows show the direction of currents.

is macroscopic (of the order of 0.1 V), already for a single capacitor: thus, it should not be difficult to build tens of centimetre-sized vacuum capacitors, wired in series, as to produce a voltage drop of volts or tens of volts. This output is far from risking to be ambiguously interpreted.

From an experimental perspective, some construction difficulties have to be faced. For example, stable ultra high vacuum required inside the capacitor may pose a technical challenge, mainly for metre-sized device. Nonetheless, vacuum technology is currently quite sophisticated and mature and we expect that the construction of light, vacuum-proof centimetre-sized capacitors should not pose any concern at all.

One issue that may be experimentally important is how the naturally present spatial thermal gradient<sup>2</sup> affects the functioning of our capacitor. Being the inner sphere made of two materials with different work functions in contact, one may expect the presence of the well known *thermocouple* (voltage/current) effect (see Fig. 8-a) that could make difficult and ambiguous the verification of the phenomenon described in this paper. As a matter of fact, the geometry of our capacitor is such that not only a macroscopic thermal gradient across the inner sphere does not affect the verification of our results (as showed in Fig. 8-b any possible thermocouple current remains confined inside the inner sphere, and the thermocouple voltage is zero being the thermocouple “shunted”), but also any thermal gradient between the outer and the inner sphere should not, since our device is, by construction, definitely not a thermocouple.

Let us now conclude anticipating (and trying to exhaustively respond to) some possible critics. Among the main objections to our results, probably

<sup>2</sup>Like that usually present inside a room between floor and ceiling.

the first one is that our device appears to suffer the same shortcomings of the self-rectifying diode scheme (see, for example, [30, Brillouin] and [31, McFee] and references therein). We have to stress that our device is quite different from a solid-state diode: in solid-state diodes physical contact, through the n-p junction, between the two terminals, and the dynamical balance between the built-in electric field and diffusion forces across the junction prevents the establishment of a non random, steady charges movement far from the depletion region toward the terminals, and thus the creation of a voltage drop between the terminal leads.

In our device, the presence of vacuum between the outer sphere and the inner one (there is no physical contact inside the capacitor), and the fact that only one sphere is covered with a low work function material, do not allow the above dynamical balance, and a definite, one-way migration of charges between plate is possible, as described above.

Another objection could be that the work function  $\phi_{ext}$  of any metallic material of which the outer sphere is made, may be high but surely not infinite: this means that a thermionic counter-emission from the outer toward the inner sphere, although very tiny, cannot be ruled out. As a matter of fact, as soon as the voltage drop is equal to the built-in potential  $\frac{\phi_{ext}-\phi_{in.}}{e}$ , the two thermionic fluxes start to counterbalance each other and no more charging of the capacitor is possible. This is true, but it does not take too much to realize that this does not weaken at all the physical essence of our approach and its challenge to the Second Law. Indeed, the specific numerical values of the output ( $V$ ,  $i$ ,  $P$ ) may be slightly different, but we do not mind: what we have provided in this paper is by itself a rough estimate.

## Acknowledgements

The author acknowledges the partial support of the Italian Space Agency under ASI Contract N° 1/015/07/0.

## References

- [1] D'Abramo, G., arXiv:0904.3188.
- [2] D. P. Sheehan (Ed.), First International Conference on Quantum Limits to the Second Law, AIP Conference Proceedings, Vol. 643, AIP Press, Melville, NY, 2002.

- [3] V. Čápek, D. P. Sheehan, Challenges to the Second Law of Thermodynamics—Theory and Experiments, Fundamental Theories of Physics, Vol. 146, Springer, Dordrecht, Netherlands, 2005.
- [4] D. P. Sheehan (Ed.), The Second Law of Thermodynamics: Foundation and Status, Proceedings of Symposium at 87th Annual Meeting of the Pacific Division of AAAS, University of San Diego, June 19–22, 2006; Special Issue of Found. Phys. 37 (2007).
- [5] L.G.M. Gordon, Found. Phys. 11 (1981) 103;  
L.G.M. Gordon, Found. Phys. 13 (1983) 989;  
L.G.M. Gordon, J. Coll. Interf. Sci. 162 (1994) 512;  
L.G.M. Gordon, Entropy 6 (2004) 38, 87, 86.
- [6] J. Denur, Am. J. Phys. 49 (1981) 352;  
J. Denur, Phys. Rev. A 40 (1989) 5390;  
J. Denur, Entropy 6 (2004) 76.
- [7] V. Čápek, J. Phys. A 30 (1997) 5245;  
V. Čápek, Czech. J. Phys. 48 (1998) 993;  
V. Čápek, Czech. J. Phys. 47 (1997) 845;  
V. Čápek, Czech. J. Phys. 48 (1998) 879;  
V. Čápek, Mol. Cryst. Liq. Cryst. 335 (2001) 24;  
V. Čápek, J. Bok, J. Phys. A 31 (1998) 8745;  
V. Čápek, Physica A 290 (2001) 379;  
V. Čápek, T. Mančal, Europhys. Lett. 48 (1999) 365;  
V. Čápek, T. Mančal, J. Phys. A 35 (2002) 2111;  
V. Čápek, D. P. Sheehan, Physica A 304 (2002) 461.
- [8] J. Bok, V. Čápek, Entropy 6 (2004) 57.
- [9] A. E. Allahverdyan, Th. M. Nieuwenhuizen, Phys. Rev. Lett. 85 (2000) 1799;  
A. E. Allahverdyan, Th. M. Nieuwenhuizen, Phys. Rev. E 64 (2001) 056117;  
A. E. Allahverdyan, Th. M. Nieuwenhuizen, Phys. Rev. B 66 (2003) 115309;  
A. E. Allahverdyan, Th. M. Nieuwenhuizen, J. Phys. A 36 (2004) 875.
- [10] Th. M. Nieuwenhuizen, A. E. Allahverdyan, Phys. Rev. E 66 (2002) 036102.
- [11] B. Crosignani, P. Di Porto, Am. J. Phys. 64 (1996) 610;  
B. Crosignani, P. Di Porto, Europhys. Lett. 53 (2001) 290;

- B. Crosignani, P. Di Porto, C. Conti, in: Quantum Limits to the Second Law, p. 267  
 B. Crosignani, P. Di Porto, C. Conti, Entropy 6 (2004) 50.
- [12] D. P. Sheehan, J. Glick, J. D. Means, Found. Phys. 30 (2000) 1227;  
 D. P. Sheehan, J. Glick, Phys. Scr. 61 (2000) 635;  
 D. P. Sheehan, J. Glick, T. Duncan, J. A. Langton, M. J. Gagliardi, R. Tobe, Found. Phys. 32 (2002) 441;  
 D. P. Sheehan, J. Glick, T. Duncan, J. A. Langton, M. J. Gagliardi, R. Tobe, Phys. Scr. 65 (2002) 430.
- [13] A. Trupp, in: Quantum Limits to the Second Law, p. 201, 231.
- [14] P. Keefe, J. Appl. Opt. 50 (2003) 2443;  
 P. Keefe, Entropy 6 (2004) 116.
- [15] J. Berger, Phys. Rev. B 70 (2004) 024524.  
 J. Berger, Physica E 29 (2005) 100.  
 J. Berger, Found. Phys. 37 (2007) 1738.
- [16] S. V. Dubonos, V. I. Kuznetsov, I. N. Zhilyaev, A. V. Nikulov, A. A. Firsov, JETP Lett. 77 (2003) 371.
- [17] A. V. Nikulov, Phys. Rev. B 64 (2001) 012505;  
 A. V. Nikulov, I. N. Zhilyaev, J. Low Temp. Phys. 112 (1998) 227.
- [18] C. Pombo, A. E. Allahverdyan, Th. M. Nieuwenhuizen, in: Quantum Limits to the Second Law, p. 254.
- [19] D. P. Sheehan, Phys. Plasmas 2 (1995) 1893;  
 D. P. Sheehan, Phys. Plasmas 3 (1996) 104;  
 D. P. Sheehan, J. D. Means, Phys. Plasmas 5 (1998) 2469.
- [20] D. P. Sheehan, J. Sci. Expl. 12 (1998) 303.
- [21] D. P. Sheehan, J. H. Wright, A. R. Putnam, Found. Phys. 32 (2002) 1557;  
 D. P. Sheehan, J. H. Wright, A. R. Putnam, A. K. Pertuu, Physica E 29 (2005) 87.
- [22] D. P. Sheehan, D. H. E. Gross, Physica A 370 (2006) 461.
- [23] D. P. Sheehan, Phys. Rev. E 57 (1998) 6660.  
 D. P. Sheehan, Physica A 280 (2001) 185.



- [24] D. P. Sheehan, J. Sci. Expl. 22 (2008) 459.
- [25] J. Earman, J. Norton, Stud. Hist. Phil. Mod. Phys. 29 (1998) 435.
- [26] Sommer, A.H.: Photoemissive materials: preparation, properties, and uses. Section 7.1, Chapter 10. *John Wiley & Sons* (1936)
- [27] Sommer, A.H.: Multi-Alkali Photo Cathode. *IRE Transactions on Nuclear Science*, pp. 8–12. Invited paper presented at Scintillation Counter Symposium, Washington, D.C., February 28-29 1956
- [28] Bates Jr., C.W., Phys. Rev. Lett. 47(3) (1981) 204.
- [29] Uebbing, J.J., James, L.W., J. Appl. Phys. 41(11) (1970) 4505.
- [30] Brillouin, J., Phys. Rev. 78(5) (1950) 627.
- [31] McFee, R., Am. J. Phys. 59 (1971) 814.
- [32] Oyama, S., Hashizume, T., Hasegawa, H. Appl. Surf. Sci. 190 (2002) 322.
- [33] Rossi, D. V., Fossum, E. R., Pettit, G. D., Kirchner, P. D., Woodall, J. M., J. Vac. Sci. Technol. B 5(4) (1987) 982.
- [34] Hsu, J. W. P., Manfra, M. J., Lang, D. V., Richter, S., Chu, S. N. G., Sergeant, A. M., Kleiman, R. N., Pfeiffer, L. N., Molnar, R. J., Appl. Phys. Lett. 78(12) (2001) 1685.
- [35] Dannhäuser, F., Solid State Electronics 10 (1967) 361.